(Received 21 September 2023, Accepted 21 November 2023, Scheduled 28 November 2023)

Hexa-Band Mobile Antenna with FSS-R-Card Combination for SAR Reduction

Guo Liu[1,*], Jie Gu[1], Zhaozhao Gao[1], Tao Tang[2,3], and Xiexun Zhang[2]

[1]*Science and Technology on Electric Information Control Laboratory, Chengdu 610036, China*
[2]*College of Electronic and Information, Southwest Minzu University, Chengdu, Sichuan 610225, China*
[3]*Key Laboratory of Electronic and Information Engineering, State Ethnic Affairs Commission, Chengdu 610041, China*

ABSTRACT: In this paper, a new SAR shield design method based on combining graphene-type absorbing cards with metal sheets via a frequency-selective surface resistive card (FSS-R-card) design is proposed. Based on this method, a low-SAR hexa-band antenna for mobile phone applications is designed. The proposed antenna has a simple structure consisting of two radiation strips and a coupling strip for enhancing the high-frequency bandwidth. The antenna covers multiple frequency bands, namely LTE Band 13 (747–787 MHz); DCS 1800 (1710–1880 MHz); PCS 1900 (1850–1990 MHz); WCDMA (1920–2170 MHz); LTE Band 40 (2300–2400 MHz); and Band 41 (2496–2690 MHz). The FSS-R-card combination acts like a PEC in the low-frequency band and like an R-card in the passband. With this approach, we were able to obtain the optimum results in reducing SAR levels and preserving the antenna efficiency in low bands. The prototype antenna was measured by the SAM head model, and measurement results show that the SAR is reduced up to 51% (at 1.9 GHz) by using the FSS-R-card. The SAR level is under 1.6 W/Kg over the whole band with good efficiency preservation at the low bands.

1. INTRODUCTION

There has been rapid growth in the design of mobile phone antennas, fueled by the number of mobile users [1–3]. Specifically, the Long-Term Evolution (LTE) bands, including LTE 13, LTE 40, and LTE 41 bands, are gaining attention in next-generation smartphone devices due to their ability to handle significantly higher data rates than the 3G bands. At the same time, the frequent use of mobile phones has led to a recent increase in public concern regarding the exposure of heads to electromagnetic radiation.

The specific absorption rate (SAR) is normally used as one of the important criteria to evaluate the degree of the hazard [4]. In the case of cellular phone services such as mobile, the SAR value must not exceed the exposure guidelines [5]. Two standards of SAR are adopted: (i) Europe uses 2 W/Kg averaged over 10 g of tissue; (ii) the U.S. Federal Communications Commission (FCC) mandates that the SAR should be lower than 1.6 W/Kg averaged over 1 g of tissue [6].

Several different methods for reducing the SAR to international standards have been proposed in recent years [7–9], and most of the SAR-reducing strategies can be roughly classified into two groups: (i) absorbing materials and (ii) reflectors. Basically, the absorbing materials can work over wider bands; however, they will lower the antenna efficiency at the same time. The reflectors (AMC, PEC, EBG, HIS. . . .) can reduce the SAR without significantly lowering the antenna efficiency; however, it is very difficult to make them work over wide bands (operation over several distinct bandwidths is needed in mobile phones). Satisfying the bandwidth, efficiency, size, and cost requirements of a low SAR solution for mobile terminals remains a challenging task.

Increasing the distance between the antenna structure and the head is the simplest way to lower the electromagnetic energy absorbed by the head. However, modern mobile handsets, which have stringent size requirements, render this solution inapplicable [10]. Using a reflector element along with the main antenna has been proposed to increase the effective radiation efficiency and reduce the SAR simultaneously [11]. Some low-SAR antenna designers have used a ferrite sheet behind the antenna, to reduce the electromagnetic fields directed to the user [12], but its main disadvantage is the cost of the material and the synthesis of the special values of permittivity and permeability that it must possess. Besides, there are also limitations in regard to the size and fragility of the ferrite for the use in mobile phones. High Impedance Surfaces (HIS), known as Artificial Magnetic Conductors (AMCs), or Electromagnetic Band Gap (EBG) structures, have also been employed to reduce the antenna SAR [13]; however, narrow-band characteristics, as well as the bulkiness of the typical EBG implementations, make it difficult to apply this approach in practical scenarios. Metamaterials have also been used as a means to reduce the SAR [14], and their drawbacks are similar to those encountered in EBG implementations. Each of these techniques appears to have its own limitations, worse, most of them ignore an important index for mobile phone antenna: radiation efficiency.

Increasing the distance between the antenna structure and the head is the simplest way to lower the electromagnetic energy absorbed by the head. However, modern mobile handsets, which have stringent size requirements, make this solution inapplicable [10]. Using a reflector element along with

* Corresponding authors: Guo Liu (liuguosgg@hotmail.com).

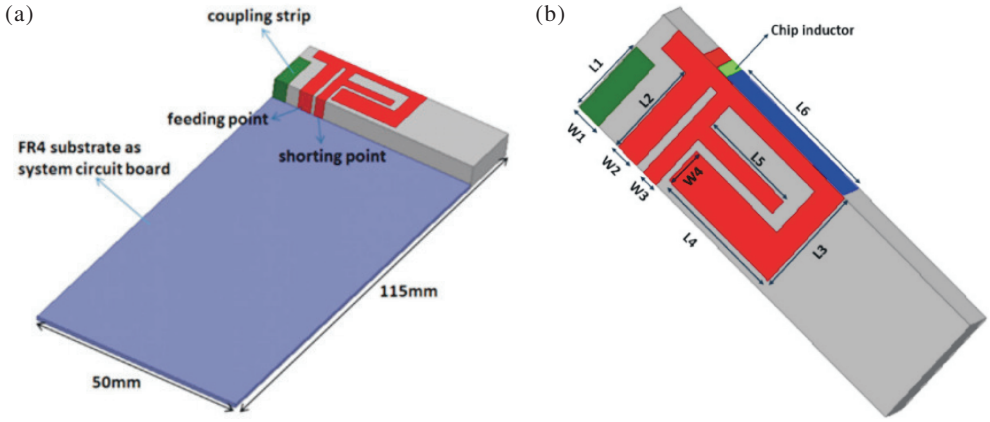

FIGURE 1. (a) Geometry of the proposed antenna. (b) Antenna dimension.

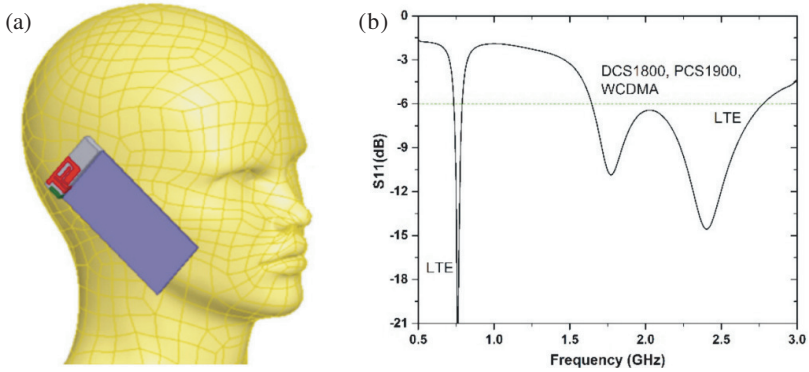

FIGURE 2. (a) Complete simulation model comprising the phone and phantom. (b) Simulated system S_{11} as a function of frequency.

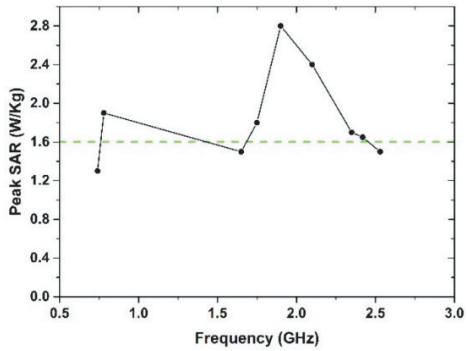

FIGURE 3. Simulated SAR as a function of frequency.

the main antenna has been proposed to increase the effective radiation efficiency and reduce the SAR simultaneously [11]. Some low-SAR antenna designers have used a ferrite sheet behind the antenna to reduce the electromagnetic fields directed to the user [12], but its main disadvantage is the cost of the material and the synthesis of the special values of permittivity and permeability that it must possess. Additionally, there are also limitations in regard to the size and fragility of the ferrite, for the use in mobile phones. High Impedance Surfaces (HIS), known as Artificial Magnetic Conductors (AMCs) or Electromagnetic Band Gap (EBG) structures, have also been employed to reduce the antenna SAR [13]; however, narrow-band characteristics, as well as the bulkiness of the typical EBG implementations, make it difficult to apply this approach in practical scenarios. Metamaterials have also been used as a means to reduce the SAR [14], and their drawbacks are similar to those encountered in EBG implementations. Each of these techniques appears to have its own limitations, and worse, most of them ignore an important index for mobile phone antenna: radiation efficiency.

Frequency selective surface (FSS) is a collection of similar unit cells in a specific order. High design versatility, compact size, multifunctional mechanism, and ease of fabrication and implementation make FSS an easy replacement for conven-

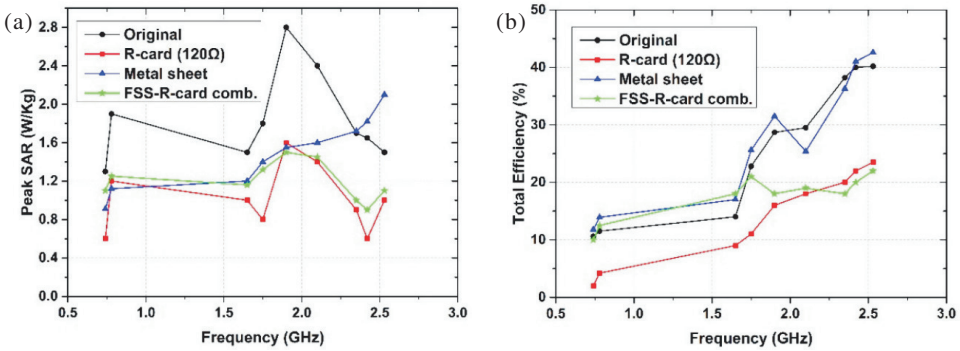

FIGURE 4. (a) Peak SAR in four different cases, (b) Total efficiency in four different cases.

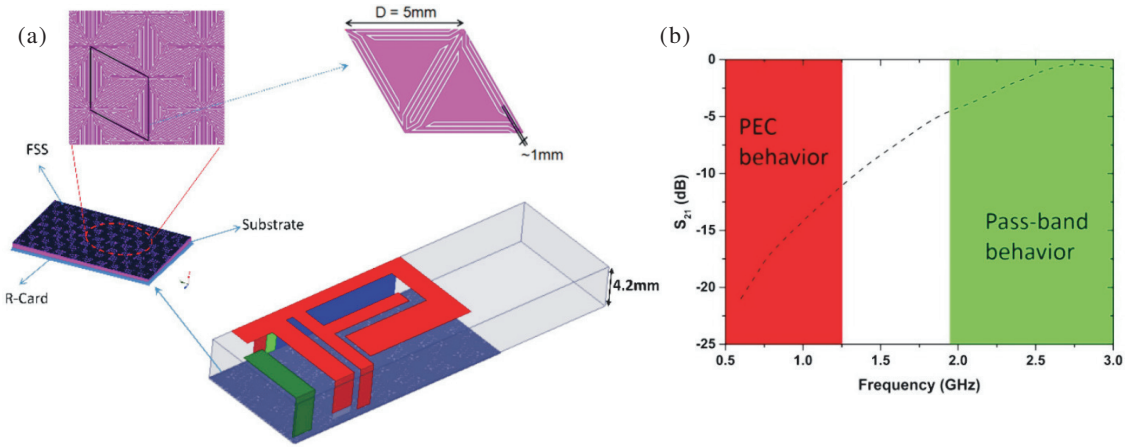

FIGURE 5. (a) FSS-R-card under the antenna ground plane. (b) S_{21} of printed FSS (3×7).

tional filters. Therefore, it exhibits special filtering characteristics [15]. Frequency-selective surface resistive card (R-card) is used to improve the antenna bandwidth [16] and to reduce the ground plane effects of an antenna at frequencies [17].

In this paper, we studied the performance of an embedded R-card implementation and a metallic sheet separately. Moreover, we combined FSS and R-card to obtain a frequency-dependent response with the best performance of the separate implementations in terms of SAR reduction and system efficiency. The FSS-R-card combination acts like a PEC in the low-frequency band and like an R-card in the high band. Details of the antenna design and measured results for the antenna performance are presented.

2. DESIGN OF ANTENNA

2.1. Antenna Configuration

The hexa-band antenna together with an imitated circuit board is shown in Fig. 1. An FR-4 substrate ($\varepsilon_r = 4.4$) is used to simulate the system board ($50 \times 115\,\text{mm}^2$), and a PEC ground plane of size $50 \times 100\,\text{mm}^2$ is printed on its backside. The proposed antenna is printed on a no-ground portion of the system circuit board of the phone and covers a small area of $15 \times 28\,\text{mm}^2$. The antenna has a simple structure comprising two radiation strips. To increase the bandwidth of the antenna at high frequency, a coupling strip is employed at the left side of the antenna (shown in Fig. 1(a)). In addition, a 9.2 nH chip inductor is used to achieve good matching at the low-band. The proposed antenna has been designed and optimized, and the final dimensions of the optimized antenna are $W1 = 3\,\text{mm}$, $W2 = 2.9\,\text{mm}$, $W3 = 2\,\text{mm}$, $W4 = 4.8\,\text{mm}$, $L1 = 9.8\,\text{mm}$, $L2 = 12\,\text{mm}$, $L3 = 13.2\,\text{mm}$, $L4 = 13.6\,\text{mm}$, $L5 = 11.8\,\text{mm}$, $L6 = 18.6\,\text{mm}$.

2.2. Problem Statement

For the numerical evaluation of SAR, we utilize a phantom model with the dispersive dielectric parameters (seen in Table 1), and the picture is shown in Fig. 2(a). The return loss (S_{11} in dB) of the antenna in the presence of the biological phantom is shown in Fig. 2(b). It is observed that the bandwidth covers the following frequency bands: LTE Band 13 (747–787 MHz), DCS 1800 (1710–1880 MHz), PCS 1900 (1850–1990 MHz), WCDMA (1920–2170 MHz), LTE Band 40 (2300–2400 MHz), and Band 41 (2496–2690 MHz). Fig. 3 shows the 1 g-average SAR distribution as a function of frequency. It is evident from the plot that the SAR exceeds the imposed standard limits around the LTE bands, as well as in the frequency range from 1.72 GHz to 2.41 GHz. The peak 1 g-average SAR values at six representative frequencies, as well as the total radiation efficiency in the presence of the biological phantom, are reported in Table 2. The presence of the biological phantom dramatically degrades the radiation efficiency of the antenna. How-

TABLE 1. Target dielectric parameters.

Frequency (MHz)	Relative Permittivity	Conductivity (S/m)
300	45.3	0.87
450	43.5	0.87
835	41.5	0.9
900	41.5	0.97
1450	40.5	1.2
1800–2000	40	1.4
2450	39.2	1.8
3000	38.5	2.4

TABLE 2. SAR and total efficiency at representative frequencies.

Frequency (GHz)	0.78	1.75	1.9	2.1	2.35	2.5
SAR (W/Kg)	1.9	1.8	2.8	2.4	1.7	1.5
Radiation efficiency (%)	11.5	22.8	28.7	29.5	38.2	46.2

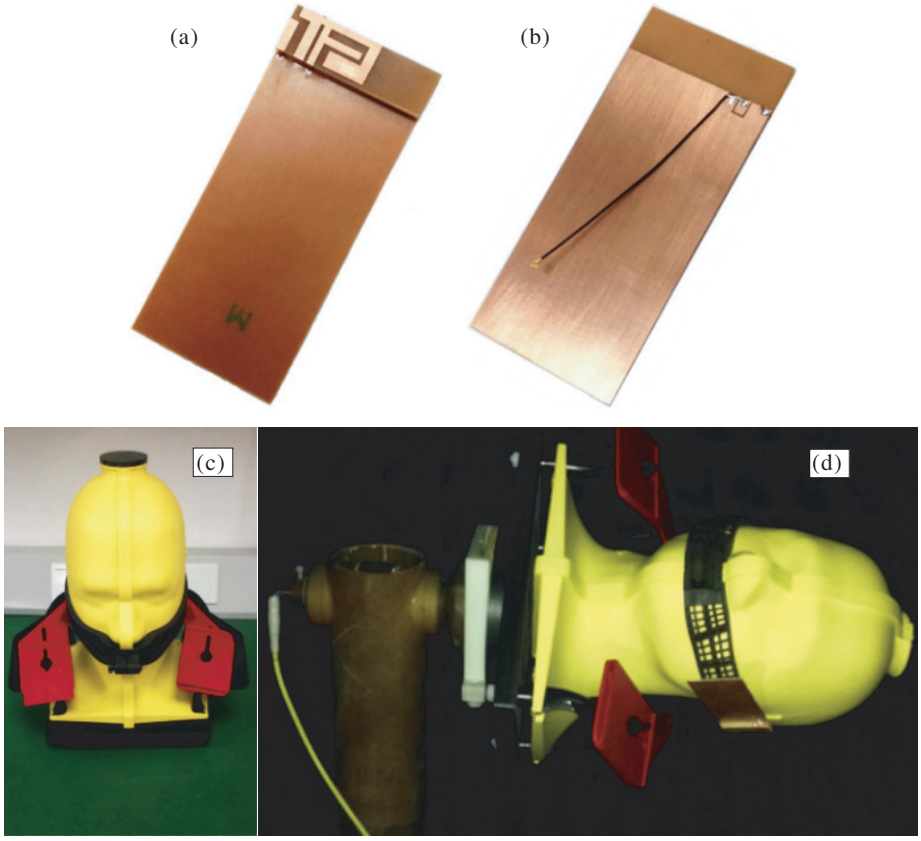

FIGURE 6. Photograph of the fabricated antenna and measurement: (a) Front view, (b) Back view, (c) SAM head model, (d) Antenna measurement in the chamber.

ever, since we are interested in showing a relative improvement in terms of SAR level reduction and efficiency preservation, we do assume the above radiation efficiency level as our reference when we apply our SAR reduction techniques.

3. RESULTS AND DISCUSSION

3.1. Metal Sheets and R-Card

In order to reduce the SAR, we tested metal sheets and R-cards of different sizes and resistivity values (ranging from 30 Ω to 300 Ω) placed between the user's head and the antenna. We learned that the resistivity value, which provides the best combined performance in terms of lowering the SAR and maintaining a good efficiency level, is 120 Ω. The results for the peak SAR and antenna efficiency are shown in Fig. 4(a) and Fig. 4(b), respectively. We note that both the graphene-based resistive card and metal sheet are effective in reducing the SAR over the lower bands. The metal sheet performs better in terms of efficiency over all bands, but the SAR exceeds the limits at high frequencies. As expected, the efficiency of the system degrades when the R-card is used (as shown in Fig. 4(b)). Specifically, the antenna efficiency at LTE Band 13 (747–787 MHz) is lower than 10%, which is unacceptable for a mobile phone system.

TABLE 3. The comparisons of antenna performance.

f (GHz)		0.78	1.75	1.9	2.1	2.35	2.5
SAR (W/Kg)	Original	2.1	1.9	3.2	2.3	1.9	1.6
	Metal sheet	***1.25***	***1.41***	***1.55***	1.51	1.72	2.1
	R-Card (120 Ω)	0.7	0.9	1.6	***1.35***	***1.02***	***1.12***
	FSS-R-card comb.	*1.21*	*1.38*	*1.57*	*1.49*	*1.25*	*1.18*
Efficiency (%)	Original	11.2	21.7	23.6	25.3	31.4	39.6
	Metal sheet	***11.9***	***23.2***	***28.5***	24.6	36.2	40.2
	R-Card (120 Ω)	2.9	11.3	16.2	***18.6***	***20.1***	***23.5***
	FSS-R-card comb.	*11.6*	*19.4*	*21.5*	*20.2*	*22.5*	*24.8*

TABLE 4. Comparison among other reported Hexa-band mobile antennas.

	Covers bands	Size (mm^2)	SAR reduction
Ref. [18]	GSM850/DCS1800/PCS1900 UMTS2100/LTE2500/LTE3600	60 × 130	N/A
Ref. [19]	LTE700/GSM850/900 Band (LB: 698–960 MHz) and the High GSM1850/1900 UMTS2100 Band (HB: 1710–2170 MHz)	50 × 120	N/A
Ref. [20]	LTE bands 42/band 43/4.9-GHz band and WLAN 2.4/5.2/5.8–GHz bands	75 × 150	N/A
Ref. [21]	CDMA 824–894 MHz; GSM 880–960 MHz; DCS 1710–1880 MHz; PCS 1850–1990 MHz; WCDMA 1920–2170 MHz; Bluetooth 2400–2484 MHz	50 × 115	Yes
Ref. [22]	LTE700/GSM850/1800/1900/UMTS/LTE2300	60 × 105	N/A
This work	LTE Band 13 (747–787 MHz); DCS 1800 (1710–1880 MHz); PCS 1900 (1850–1990 MHz); WCDMA (1920–2170 MHz); LTE Band 40 (2300–2400 MHz); and Band 41 (2496–2690 MHz)	50 × 115	Yes

3.2. Design of FSS-R-Card

In order to combine the metal-sheet performance over the lower bands with that of the R-card at high frequency, we printed a high-pass FSS and placed an R-card of the same size directly below it (as shown in Fig. 5(a)).

The transmission coefficient of the utilized FSS sheet is shown in Fig. 5(b). The thickness of the sub-PCB used as a substrate is 0.8 mm with a relative permittivity of $\varepsilon_r = 4.4$ and $\tan(\delta) = 0.02$. The S_{21} of the FSS printed over the substrate shows a passband from 1.92 GHz and acts like a PEC ($S_{21} < -10$ dB) below 1.25 GHz. If an R-card of the same size (15 mm × 28.5 mm) is placed directly below the sub-PCB, a reflecting behavior is obtained at low frequency and an absorbing one over the higher band. The SAR and efficiency performance (Figs. 4(a) and 4(b)) confirm our predictions regarding the behavior of the FSS-R-card combination. The performance of the FSS in terms of both efficiency and SAR levels was closer to the metal at low frequency and to the R-card at high frequency, as desired. Moreover, this solution has extremely low profile, as the metal FSS is printed over a substrate already present in the mobile phone. Thus, this solution can be modeled on any phone without altering its structure or adding bulkiness. Due

to its special performance, the FSS-R-card structure proposed in this paper has many potential applications, such as radomes and energy-selective surfaces.

3.3. Measured Results

The proposed hexa-band antenna has been successfully implemented and measured. Pictures of the prototype are shown in Figs. 6(a) and (b). The measurements are carried out by using an Agilent 8753ES vector network analyzer in the Airlinklab system. In order to test the SAR value, the antenna is placed in a tilted position relative to the SAM-V4.5BS head phantom (as shown in Figs. 6(c) and (d)). The head phantom is filled with a broadband head tissue-simulating gel for OTA evaluation. It can work at 0.3–6 GHz. The measured S_{11} of the proposed antenna is given in Fig. 7. It shows that the proposed FSS-R-card structure does not have an obvious influence on the resonant frequency, and the antenna can work well at all interested bands. To observe the antenna performance clearly, the comparisons of the results are listed in Table 3. It can be seen that the SAR is reduced up to 51% (at 1.9 GHz) by using the FSS-R-card combination. The SAR level is under 1.6 W/Kg over the whole band with good efficiency preservation at the low bands. The FSS-R-card combination can achieve a better trade-off between SAR level reduction and efficiency preservation than other strategies. Table 4 compares the proposed hexa-band mobile antenna with the FSS-R-card with other reported ones.

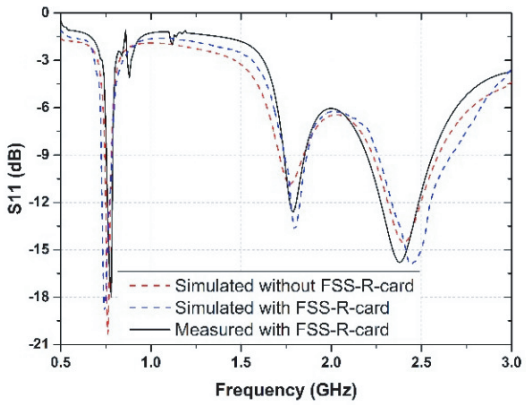

FIGURE 7. The Comparisons of Antenna Performance.

4. CONCLUSIONS

A novel mobile phone antenna has been achieved for hexa-band operation, and an FSS-R-card combination for SAR reduction has been proposed and successfully implemented. In this study, the proposed design is able to provide frequency-dependent performance, utilizing the effects of a metal sheet or of an absorbing material when necessary, over a wide frequency range. Results show that the FSS-R-card combination can achieve a better trade-off between SAR level reduction and efficiency preservation than other strategies. This solution can be directly embedded into the mobile phone by using its pre-existing parts as substrates, thus requiring no additional space. The proposed antenna has a small size ($15 \times 28\,\text{mm}^2$) with good performance in the whole interested bands, which makes it very useful in next-generation wireless communication systems.

REFERENCES

[1] Lu, J.-H. and J.-L. Guo, "Small-size octaband monopole antenna in an LTE/WWAN mobile phone," *IEEE Antennas and Wireless Propagation Letters*, Vol. 13, 548–551, 2014.

[2] Wang, Z., L. Z. Lee, D. Psychoudakis, and J. L. Volakis, "Embroidered multiband body-worn antenna for GSM/PCS/WLAN communications," *IEEE Transactions on Antennas and Propagation*, Vol. 62, No. 6, 3321–3329, Jun. 2014.

[3] Ban, Y.-L., Y.-F. Qiang, Z. Chen, K. Kang, and J. L.-W. Li, "Low-profile narrow-frame antenna for seven-band WWAN/LTE smartphone applications," *IEEE Antennas and Wireless Propagation Letters*, Vol. 13, 463–466, 2014.

[4] Messaoudi, H. and T. Aguili, "SAR reduction in the human head model using metamaterials," in *2019 IEEE 19th Mediterranean Microwave Symposium (MMS 2019)*, 1–5, Hammamet, Tunisia, Oct. 2019.

[5] Ahlbom, A., U. Bergqvist, J. Bernhardt, J. Cesarini, L. Court, M. Grandolfo, M. Hietanen, A. McKinlay, M. Repacholi, D. Sliney, J. Stolwijk, M. Swicord, L. Szabo, M. Taki, T. Tenforde, H. Jammet, R. Matthes, and I. C. N. R. Protectio, "Guidelines for limiting exposure to time-varying electric, magnetic, and electromagnetic fields (up to 300 GHz)," *Health Physics*, Vol. 74, No. 4, 494–522, Apr. 1998.

[6] IEEE Std C95.1-1991, "IEEE standard for safety levels with respect to human exposure to radio frequency electromagnetic fields, 3 KHz to 300 GHz," 1–76, 1992.

[7] Bang, J. and J. Choi, "A SAR reduced mm-wave beam-steerable array antenna with dual-mode operation for fully metal-covered 5G cellular handsets," *IEEE Antennas and Wireless Propagation Letters*, Vol. 17, No. 6, 1118–1122, Jun. 2018.

[8] Wang, M., Z. Yang, J. Wu, J. Bao, J. Liu, L. Cai, T. Dang, H. Zheng, and E. Li, "Investigation of SAR reduction using flexible antenna with metamaterial structure in wireless body area network," *IEEE Transactions on Antennas and Propagation*, Vol. 66, No. 6, 3076–3086, Jun. 2018.

[9] Singh, S. and S. Verma, "SAR reduction and gain enhancement of compact wideband stub loaded monopole antenna backed with electromagnetic band gap array," *International Journal of RF and Microwave Computer-Aided Engineering*, Vol. 31, No. 10, Oct. 2021.

[10] Takagi, K., Y. Furukawa, Y. Koyamashita, S. Kusunoki, and S. Tsuchiya, "Portable telephone with reduced specific absorption rate and improved efficiency," U.S. Patent 7,274,953 B2., Sep. 2007.

[11] Hirata, A., T. Adachi, and T. Shiozawa, "Folded-loop antenna with a reflector for mobile handsets at 2.0 GHz," *Microwave and Optical Technology Letters*, Vol. 40, No. 4, 272–275, Feb. 2004.

[12] Lu, B., B. Pang, W. Hu, and W. Jiang, "Low-SAR antenna design and implementation for mobile phone applications," *IEEE Access*, Vol. 9, 96 444–96 452, 2021.

[13] Zhang, H. H., G. G. Yu, Y. Liu, Y. X. Fang, G. Shi, and S. Wang, "Design of low-SAR mobile phone antenna: Theory and applications," *IEEE Transactions on Antennas and Propagation*, Vol. 69, No. 2, 698–707, Feb. 2021.

[14] Mahmood, S. N., A. J. Ishak, T. Saeidi, H. Alsariera, and A. Soh, "Recent advances in wearable antenna technologies: A review," *Progress In Electromagnetics Research B*, Vol. 89, 1–27, 2020.

[15] Katoch, K., N. Jaglan, and S. D. Gupta, "A review on frequency selective surfaces and its applications," 75–81, NOIDA, India,

2019.

[16] Wang, J., S. Liu, J. Lou, and X. Zhao, "Ultra-wideband array with multi-layer frequency selective surface resistive-card and 51.4 : 1 bandwidth," 1–3, Qingdao, China, 2023.

[17] Johnson, A. D., J. Zhong, S. B. Venkatakrishnan, E. A. Alwan, and J. L. Volakis, "Phased array with low-angle scanning and 46 : 1 bandwidth," *IEEE Transactions on Antennas and Propagation*, Vol. 68, No. 12, 7833–7841, Dec. 2020.

[18] Alja'afreh, S. S., Y. Huang, Q. Xu, and L. Xing, "Hexa-band antenna for smartphone applications," in *2017 10th Jordanian International Electrical and Electronics Engineering Conference (JIEEEC)*, 1–4, Amman, Jordan, May 2017.

[19] Zheng, M., H. Wang, and Y. Hao, "Internal hexa-band folded monopole/dipole/loop antenna with four resonances for mobile device," *IEEE Transactions on Antennas and Propagation*, Vol. 60, No. 6, 2880–2885, Jun. 2012.

[20] Peng, M., H. Zou, Y. Li, M. Wang, and G. Yang, "An eight-port 5G/WLAN MIMO antenna array with hexa-band operation for mobile handsets," in *2018 IEEE Antennas and Propagation Society International Symposium on Antennas and Propagation & USNC/URSI National Radio Science Meeting*, 39–40, Boston, Ma, Jul. 2018.

[21] Peng, C.-M., I.-F. Chen, and C.-T. Chien, "A novel hexa-band antenna for mobile handsets application," *IEEE Transactions on Antennas and Propagation*, Vol. 59, No. 9, 3427–3432, Sep. 2011.

[22] Wang, L., W. Lin, and G. Yang, "An internal hexa-band antenna for 4G mobile phone application," in *2013 IEEE International Conference on Microwave Technology & Computational Electromagnetics (ICMTCE)*, 239–241, Qingdao, China, Aug. 2013.